# THE 36-CELL STRUCTURE – CALCULATIONS AND EXPERIMENTS

P. Hülsmann, W.F.O. Müller and H. Klein,
Institut für Angewandte Physik, Universität Frankfurt am Main, Germany
U. van Rienen and T. Weiland,
Theorie Elektromagnetischer Felder, Technische Hochschule Darmstadt, Germany

*Abstract*

The wake field effects in accelerator sections for future linear colliders will be reduced either by damping, by detuning or a combination of both. In the case of the DESY S-Band Test Facility [1] it is foreseen to employ two higher order mode (HOM) damped cells within a detuned stack of undamped ones. In order to obtain optimal performance by use of single cell dampers a design was derived by applying numerical tools. To understand the behaviour of such a damper cell in a detuned structure, a damper cell was build and inserted in a strongly detuned 36-cell S-Band structure. This structure was investigated by bead pull measurements. The predictions of MAFIA field calculations were compared to experimental results.

## 1 INTRODUCTION

The S-Band 500 GeV Linear Collider Study SBLC foresees about 5000 constant gradient (cg) acceleration structures of 180 cells with a loaded gradient of 17 MV/m. It considers a bunch train of 333 bunches with a spacing of 6 ns from bunch to bunch. To achieve a high luminosity any cumulative beam break up along the bunch train has to be avoided. Wakefield effects driven by HOMs are one of the primary sources of emittance growth. Consequently, the suppression of these HOMs is a very crucial point in all actual linear collider designs. The major interest of calculations was focused on the modes of the first dipole band since they cause the severest deflecting effects, but also the $3^{rd}$ and $6^{th}$ dipole passband need to be studied.

Calculations for the SBLC structure were carried out with ORTHO [2] for a somewhat simplified 180-cell structure with 30 landings. One of the main results was that not only the first $\pi$-like dipole modes influence the beam dynamics but about 140 modes! A major part of these deflecting modes is trapped inside the cg structure, that is without contact to the end cells.

Since the phenomenon of trapped HOMs in tapered waveguides was neither theoretically nor experimentally well known and has a strong influence on the design of damping schemes further HOM investigations have been started: A test structure was designed with the goal to have a structure which is easy to measure, easy to manufacture, which is computable with different numerical methods (MAFIA, URMEL–T, ORTHO, COM) without geometric approximations, and which shows the clear appearance of trapped modes.

Performing RF-measurements on long structures is severely limited by the appearance of mode overlap. Therefore a relatively short structure had to be chosen. In order to get a both mechanically and thermally stable structure a massive design was chosen. For low mechanical tolerances a simple geometry was designed. The structure has a very strong linear tapering of the iris, constant outer radius and twice as thick irises as the original SBLC structure. Comparisons of numerical calculations and measurements without damping system [3], gave a good agreement in resonance frequencies and the field distribution. Further the clear appearance of trapped modes was found for several modes [4]. Calculations for the damped system have also been done, and have been compared with measurements.

## 2 THE TEST SETUP

The structure, made of standard OFHC copper, consists of 36 cells clamped together by truss rods. The cell geometry is similar to the one chosen for the SBLC, except for the iris thickness which is 10 mm instead of 5 mm. The iris openings were evenly tapered from 40 mm diameter at the beginning to 20 mm at the end.

For the measurements of the damped structure we have inserted a sheet of paper covered with graphite in cell #18. This damping material could be inserted without demounting of the structure. It is only a model for test purposes that represents a damping unit like a wall slotted cell with four rectangular waveguides attached. This method avoids the influence of changed electrical contacts due to the reassembling on the measured Q-values. Proper alignment is ensured by laying the structure on top of an optical bench. The field measurements were performed using a modified nonresonant bead pull technique [5], [6], [7]. Data is taken by a HP8719c network analyser for 801 discrete positions along several paths parallel to the cavity axis.

## 3 SIMULATION WITH DAMPING SHEET

The simulation of the 36-cell structure with a very thin (about 1.5 μm) damping sheet in cell #18 is practically not possible with discretization methods since it is not possible to mesh accurately enough within reasonable storage demands. Therefore other methods were necessary to get quantitative theoretical results for the damping effect. In case of small losses it is well known that the field distribution does not change considerably compared with the loss free case. Then it is reasonable to use the field distribution of the loss free case to calculate the power loss by means of perturbation theory. As the measurement improved [4] the undisturbed field distribution may be used to calculate the damping effect for the 36-cell structure.

0-7803-4376-X/98/$10.00 © 1998 IEEE

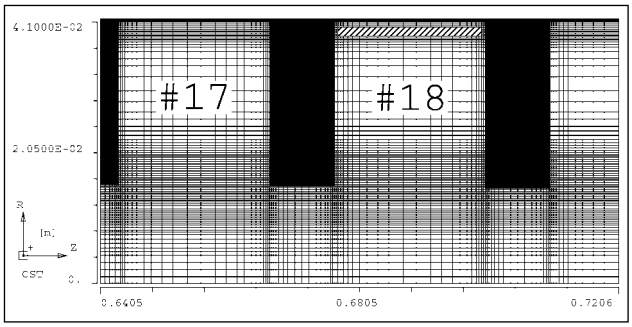


Figure 1: Three cells out of the 36-cell structure. Cell #18 with the damping material (hatched).

Practically this was done with MAFIA in the following way: First a loss free field calculation was executed for the original 36-cell structure. In a second calculation a thin sheet with a different material number was inserted in cell #18, as shown in figure 1. The hatched area near the outer wall of cell #18 is the graphite. Even though a rather coarse mesh would lead to a perfect approximation of the structures shape[1] preceding studies showed that smaller step sizes near all edges resulted in much better agreement for the frequencies obtained in measurement respective simulation while the field distribution agrees already well enough for a coarse, quasi equidistant mesh. The frequency is very sensitive to an appropriate discretization and an appropriate bead [3].

During the solution of the eigenvalue problem this material as well as all walls of the structure are treated as perfect conductors. Afterwards, in the postprocessing all wall material gets the conductivity of copper $\sigma = 5.8 \cdot 10^7$ S/m while the sheet in cell #18 gets a lower conductivity.

At this point some approximations are necessary since the sheet has to be thicker than the original one from the measurements. The reasons are that each material should be discretized with at least two steps in each coordinate direction and that the quotient of largest to smallest step size should be kept within reasonable limits in order to limit the condition number of the matrix of the eigenvalue problem. Therefore the material sheet which represents the very thin graphite sheet got a conductivity of $\sigma = 5.0 \cdot 10^6$ S/m instead of graphite's conductivity of $\sigma = 1.25 \cdot 10^5$ S/m.

After calculating the total stored energy $W_{tot}$ and the wall losses[2] $P_{wall}$ the quality factor $Q$ may be determined [8] for a mode with frequency $\omega$ by

$$Q = \omega \cdot \frac{W_{tot}}{P_{wall}} . \qquad (1)$$

Finally the frequency shift caused by the damping sheet in cell #18 is obtained by (2) neglecting second order terms.

$$\frac{\delta\omega}{\omega_0} = \frac{1}{2Q} \qquad (2)$$

1. i. e. vanishing geometric error
2. by power loss method

## 4 THE MEASUREMENT METHOD

The method applied is a variant of the nonresonant bead-pull technique as described elsewhere [9]. In the measurements we are only interested in the longitudinal component of the electric field, because it is sufficient to indicate the effect of the damper cell. Thus we used a dielectric needle ($Al_2O_3$, $\varepsilon_r = 9.2$) as bead. This ceramic bead was 6 mm long and 1 mm in diameter. A lumped circuit representation of the resonator combined with Slaters formula [10] leads to the electric field:

$$E^2 = \frac{P_{wall}}{\alpha} \cdot \frac{(1 + k_1 + k_2)^2}{2\omega \cdot \sqrt{k_1 k_2}} \cdot |\Delta s_{21}| \qquad (3)$$

## 5 RESULTS

For the measurements the bead was calibrated in a $TM_{010}$-pillbox for the longitudinal perturbation constant ($\alpha = 9.34 \cdot 10^{-20}$ Asm$^2$/V). Since the measured modes were of dipole type the bead pull measurements were performed off-axis with a distance of 7 mm to the structures axis. For the measurements we have chosen several modes of the first dipole passband which have significant field strength at the damper position (cell #18) since a considerable damping effect could only be expected in this case.

In a tapered structure trapped modes always change their phase shift from cell to cell from 0 to $\pi$. To investigate the influence of the damper position, we have chosen mode A with the $\pi$-end, mode B with the $\pi/2$-part and mode C with the 0-end at the damper position. Additionally all modes between A and C have been measured (see figure 2). The results are summarized in table 1.

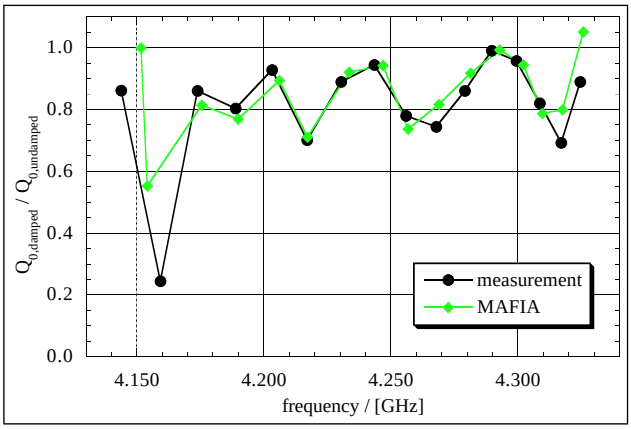


Figure 2: Comparison of calculated and measured damping effect (reduction of $Q_0$).

As mentioned above, the damper was realized by a sheet of paper covered with graphite (thickness 1.5 µm, conductance of graphite = $1.25 \cdot 10^5$ 1/Ωm). First the sheet was pressed to the inner wall of cell #18 in order to have a symmetric damper and relatively weak damping effect (damper on surface). Additionally the damping effect was increased by moving the sheet some mm towards the iris, since the

electrical field increases in this direction (damper in cell). The results of simulations are presented in table 2. It must be mentioned, that Q-values calculated by the simulations are always higher than those derived by measurements. This is caused by HF-contacts between adjacent copper cells.

To compare the results from measurements and calculations, damping effect versus frequency is plotted for both in figure 2. As can be seen there the agreement is mostly excellent, except the first two modes on the left. These two modes proofed to be very sensitive on the position of the π-like end. Already a small disturbance moves the position to the next cell. Thus this discrepancy was expected.

Table 1: Measurement results

| $f_0$ [GHz] | $Q_{0,undamp.}$ | $Q_{0,damped}$ | $Q_{0,d.}/Q_{0,und.}$ |
|---|---|---|---|
| 4.143,830 | 10,353 | 8,927 | 0.862 |
| 4.159,260 | 10,264 | 2,507 | 0.244 |
| 4.173,972 | 10,464 | 9,002 | 0.860 |
| 4.188,848 | 10,157 | 8,161 | 0.803 |
| 4.203,234 | 10,193 | 9,454 | 0.928 |
| 4.217,087 | 11,291 | 7,919 | 0.701 |
| 4.230,494 | 10,848 | 9,646 | 0.889 |
| 4.243,603 | 10,997 | 10,389 | 0.945 |
| 4.256,029 | 10,490 | 8,181 | 0.780 |
| 4.267,888 | 11,174 | 8,319 | 0.744 |
| 4.279,207 | 11,185 | 9,621 | 0.860 |
| 4.289,655 | 11,447 | 11,350 | 0.991 |
| 4.299,424 | 11,396 | 10,923 | 0.958 |
| 4.308,621 | 11,757 | 9,640 | 0.820 |
| 4.317,108 | 11,918 | 8,244 | 0.692 |
| 4.324,609 | 12,112 | 10,764 | 0.889 |

## 6 CONCLUSION

From former measurements a strong influence on mode geometry was expected [11]. But weak damping as well as strong damping has not changed the mode geometry significantly. The damping effect is evenly distributed over all phase shifts.

The black line in figure 2 represents the measurement results for the Q-reduction. The results of the MAFIA calculations are plotted as gray line. For all modes, except the first two ones, an excellent agreement was found. Thus one may say that the numerical representation of the damper was successful.

Table 2: Results from MAFIA-calculation

| $f_0$ [GHz] | $Q_{0,undamp.}$ | $Q_{0,damped}$ | $Q_{0,d.}/Q_{0,und.}$ |
|---|---|---|---|
| 4.151,653 | 13,650 | 13,645 | 1.000 |
| 4.154,160 | 12,552 | 6,936 | 0.553 |
| 4.175,661 | 12,641 | 10,291 | 0.814 |
| 4.189,950 | 12,736 | 9,785 | 0.768 |
| 4.206,170 | 12,839 | 11,478 | 0.894 |
| 4.217,273 | 12,947 | 9,205 | 0.711 |
| 4.233,617 | 13,066 | 12,032 | 0.921 |
| 4.246,928 | 13,185 | 12,426 | 0.942 |
| 4.256,809 | 13,308 | 9,809 | 0.737 |
| 4.268,974 | 13,436 | 10,972 | 0.817 |
| 4.281,471 | 13,570 | 12,449 | 0.917 |
| 4.292,834 | 13,699 | 13,596 | 0.992 |
| 4.302,226 | 13,833 | 13,064 | 0.944 |
| 4.309,774 | 13,962 | 10,984 | 0.787 |
| 4.317,561 | 14,094 | 11,269 | 0.800 |
| 4.325,724 | 14,229 | 14,953 | 1.051 |

## 7 REFERENCES


[1] N Holtkamp: “The S-Band Linear Collider Test Facility“, this conference

[2] U. van Rienen: “Higher Order Mode Analysis of Tapered Disc–Loaded Waveguides using the Mode Matching Technique“, Particle Accelerators, Vol. 41, pp. 173 - 201, 1993

[3] M. Kurz et al.: “Higher Order Modes in a 36-Cell Test Structure“, 5th EPAC, Barcelona, 1996

[4] W.F.O. Müller, P. Hülsmann, M. Kurz, C. Peschke, H. Klein, U. van Rienen, T. Weiland, M. Dohlus: “Measurements and Numerical Calculations on Higher Order Mode Dampers“; Proceedings of the XVIII$^{th}$ International Linac Conference, Geneva (Switzerland), Aug. 1996

[5] C.W. Steele: “A Nonresonant Perturbation Theory“, IEEE Trans. MTT-14 (2), pp. 70-74, 1966

[6] P. Hülsmann, M. Kurz, H. Klein: “Experimental Determination of Field Strength and Quality Factor of heavily damped Accelerator Cavities“, Electronics Letters, Vol. 27 No. 19, pp. 1727-1729, 12.09.1991

[7] M. Kurz: “Untersuchungen zu mikrowellenfokussierenden Beschleunigerstrukturen für zukünftige lineare Collider“, thesis, Frankfurt, 1993

[8] T. Weiland: “High Precision Eigenmode Computation“; Particle Accelerators, Vol. 56, pp. 61-82, 1996

[9] B. Krietenstein et al.: “The S-Band 36-Cell Experiment“, Particle Accelerator Conference and International Conference on High-Energy Accelerators, Dallas (Texas), 1995

[10] L.C. Maier, J.C. Slater: “Field Strength Measurements in Resonant Cavities“, Journal of Applied Physics, 23 (1), 1952

[11] M. Dohlus et al.: “S-Band HOM-Damper Calculations and Experiments“, Particle Accelerator Conference and International Conference on High-Energy Accelerators, Dallas (Texas), 1995



**(work supported by DESY / Hamburg and BMBF under contract 06of359)**